Volume 80, Issue 1

ISSN 0260-8774

ELSEVIER

journal of food engineering

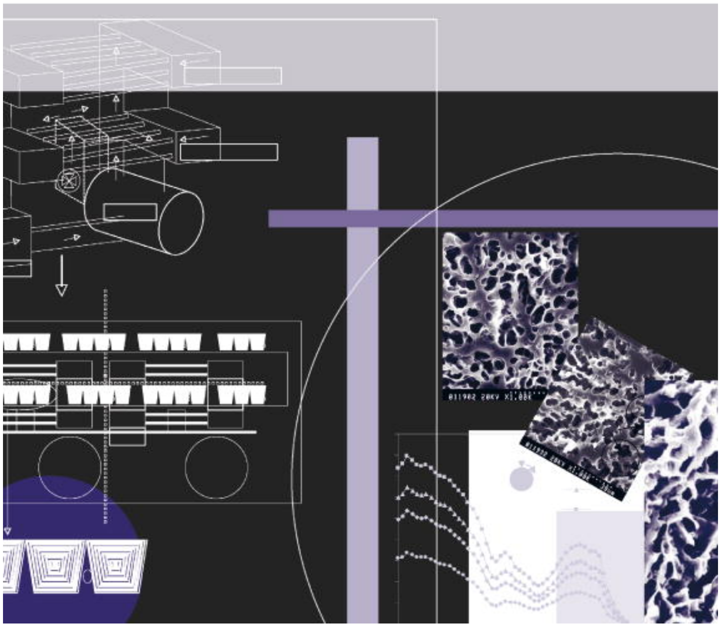

Available online at www.sciencedirect.com
ScienceDirect
Journal of Food Engineering 80 (2007) 11–17
JOURNAL OF FOOD ENGINEERING
www.elsevier.com/locate/jfoodeng

A poroelastic model for wave propagation in partially frozen orange juice

José M. Carcione [a,1], Osvaldo H. Campanella [b,*], Juan E. Santos [c,d]

[a] *Istituto Nazionale di Oceanografia e di Geofisica Sperimentale (OGS), Borgo Grotta Gigante 42c, 34010 Sgonico, Trieste, Italy*
[b] *Department of Agricultural and Biological Engineering and Whistler Center for Carbohydrates Research, Purdue University, West Lafayette, IN 47907, USA*
[c] *CONICET and Facultad de Ciencias Astronómicas y Geofísicas, Universidad Nacional de la Plata Paseo del Bosque, 1900 La Plata, Argentina*
[d] *Department of Mathematics, Purdue University, 150 N. University Street, IN 47907-2067, USA*

Received 10 August 2004; received in revised form 25 February 2006; accepted 18 April 2006
Available online 12 May 2006

Abstract

We use a poroelastic model to describe the propagation of ultrasonic waves through orange juice, which is subjected to a freezing process. The theoretical results are compared with those obtained by ultrasound methods used to monitor the freezing of orange juice. The ultrasonic properties of partially frozen orange juice, specifically, are characterized by the P-wave and S-wave velocities and their respective attenuation coefficients, which are related to the amount of water in the juice in the liquid state. Kelvin's model is used to obtain the amount of unfrozen water in the juice as a function of temperature, and the Biot's poroelastic theory provides the ultrasonic properties of orange juice as a function of temperature, below the eutectic point. A model similar to the Kelvin's model is used in the food literature to describe the crystallization of ice as a function of temperature. In concurrence with the Kelvin's model describing the formation of ice crystals, the frame moduli of the ice-crystal matrix are obtained by a percolation model of ice formation. The model shows a good agreement with the experimental data, regarding the wave velocities, and a qualitative agreement with the experimental attenuation values. A critical temperature, at nearly 50% saturation, is related to the maximum attenuation of the fast P-wave, and maximum velocity and minimum attenuation of the slow P-wave.

Keywords: Frozen orange juice; Poroelastic model; P-waves; S-waves; Velocity; Attenuation

1. Introduction

Ultrasound is currently used to evaluate the quality of foods (McClements et al., 1987; Povey & Mason, 1995; Povey, 1997). The technique uses the P-wave and S-wave velocities and respective attenuation factors to verify and monitor the state of foods, such as fruit ripeness, fat content in oils and degree of freezing (Miles & Cutting, 1974). In particular, monitoring the freezing of foods is important for quality purposes because the freezing process may damage the structure of foods and consequently affect their quality due mainly to the increase in size of the ice crystals after nucleation. Recently, Sigfusson, Ziegler, and Coupland (2004) Lee, Pyrak-Nolte, Cornillon, and Campanella (2004) have performed ultrasound experiments on gelatine gels, muscle proteins and orange juice at frequencies of 2.5 MHz and 5 MHz respectively and for a range of temperatures. Sigfusson et al. (2004) measured P velocities of the ultrasound waves through the gels and muscle proteins whereas Lee et al. (2004) measured P- and S-waves velocities and P-wave attenuation of freezing orange juice, which showed a strong correlation with the

* Corresponding author. Fax: +1 765 4961115.
E-mail addresses: jcarcione@ogs.trieste.it (J.M. Carcione), campa@purdue.edu (O.H. Campanella), santos@fcaglp.fcaglp.unlp.edu.ar (J.E. Santos).
[1] Fax: +39 040 327521.

0260-8774/$ - see front matter
doi:10.1016/j.jfoodeng.2006.04.044

amount of unfrozen water in the juice. Specifically, for orange juice, the experimental data showed a strong velocity increase below −10 °C and an attenuation peak at −20 °C, in correspondence with a proportion of unfrozen water in the juice of nearly 20%.

We use a poroelastic model to describe the wave propagation phenomenon and to obtain the wave velocities and attenuation factors of partially frozen orange juice. Biot developed a theory of propagation of elastic waves in porous media, where the two-phase material is considered as a continuum, thus ignoring the microscopic level (Biot, 1956, 1962; Carcione, 2001). Within this context, the macroscopic variables follow the laws of continuum mechanics. Basically, the theory assumes that anelastic effects arise from viscous interactions between the fluid and the solid. The assumptions of the theory are the following: (i) the wavelength of the propagating wave is large in comparison with the dimensions of the pores. This is a requirement for applying the theory of continuum mechanics, and implies that scattering dissipation is neglected. (ii) Displacements are small, so that the macroscopic strain tensor is related to the displacements by the nearest second order approximation. (iii) The liquid phase is continuous, implying that pores are connected and that disconnected pores are part of the matrix frame, and (iv) the medium is isotropic and fully saturated.

With this theory Biot demonstrated the existence of two kinds of compressional (P) modes in a porous medium: a fast P-wave in which the solid and the fluid displacements are in phase, and a slow P-wave in which the displacements of the liquid and the solid are out of phase. At low frequencies, the medium does not support the slow wave, which becomes diffusive, since the fluid viscosity effects dominate (a thick boundary layer compared to the pore size). At high frequencies, tangential slip takes place (thin boundary layer), the inertial effects are predominant and the slow mode may have a wave-like character. This wave contributes to the attenuation of the fast wave by mode conversion at inhomogeneities.

The amount of unfrozen water in the juice was related to the temperature by means of the Kelvin's model (Hudson, 1992), which is similar to a model used to describe ice formation in frozen foods (Karel & Lund, 2003). Use of Biot's model requires the moduli of the dry matrix, which are obtained by a percolation model (Arbabi & Sahimi, 1988; Leclaire, Cohen-Ténoudji, & Aguirre-Puente, 1994). The high-frequency flow of the liquid is described by a viscodynamic correction on the basis of the dynamic tortuosity obtained by Johnson, Koplik, and Dashen (1987) (see also Carcione, 2001).

2. Poroelastic model

By applying Biot's theory (Biot, 1956, 1962; Carcione, 2001) to orange juice during the freezing process, we assume that the solid phase is frozen water, and the liquid phase is the unfrozen juice. We neglect the presence of solid particles (pulp) at the initial (unfrozen) state, although their presence may cause a freezing point depression, as can be seen in the experimental data reported by Lee et al. (2004). Hereafter, ice and water will indicate the frozen and liquid juice, respectively.

2.1. Water proportion versus temperature

In order to interpret the experimental results of Lee et al. (2004), let us clarify the concepts of initial freezing temperature and eutectic point for the freezing of orange juice. Orange juice can be thought as to be a solution of approximately 10% non-fat polysaccharides (essentially soluble solids) in water. At ambient temperature, there will only be one phase present, i.e. the solution. If we cool down the solution, pure ice will form at the initial freezing temperature of that solution, usually less than 0 °C because the initial freezing point is depressed by the presence of the solute. Upon freezing ice is formed. Intermolecular forces such as van der Waals interactions, electrical forces and hydrogen bonding determine the strength of the formed ice lattice. The presence of solute breaks up the regular pattern of the lattice and decreases the freezing or melting temperature. In general, the greater the concentration of solutes, the more the freezing point will be depressed. If we continue to lower the temperature and more ice is formed, we are essentially removing water from the solution so the solute concentration in the solution increases thus lowering further the freezing point of the solution. It is important to note that for food materials freezing occurs in a range of freezing temperatures. By lowering the temperature still further we finally approach the eutectic temperature. At this point, the solute concentration in the juice reaches a maximum and the unfrozen liquid that contains the solute starts to freeze as a non-pure ice mixture. However, due to viscosity effects, it is unlikely that the solute will crystallize at the eutectic temperature and the freeze-concentration process may proceed beyond this point.

Thus, the mass fraction of the unfrozen juice, related to the mass fraction of the ice formed, is extremely important to describe the system. Several approaches have been used to estimate the amount of ice (or the amount of unfrozen juice) as a function of the temperature. An approach is based on an equation that is derived from the colligative properties of binary solutions, specifically the decrease of the freezing point of a binary solution (Singh, 1995) due to the presence of the solute. That equation, however, has to be corrected by the amount of unfreezable water, a parameter that is very difficult to measure and has been the object of considerable debate. Therefore, we preferred using an equation to estimate the crystallization of ice particles (Karel & Lund, 2003). That equation has also been used to describe the crystallization of ice cream (Hartel, 1998). The equation is similar to the Kelvin's equation that relates the equilibrium of a liquid drop to its radius of curvature r at constant external pressure (Hudson, 1992). By considering the formation of ice crystals the equation can be written as:

$$\ln\left(\frac{T}{T_0}\right) = -\frac{2\sigma}{r}\left(\frac{V}{\Delta H_{\mathrm{F}}}\right) \tag{1}$$

where T is the melting temperature of an ice particle of radius r, T_0 is the freezing point of a flat ice particle, σ is the interfacial free energy between the ice and the surrounding liquid, V is the molar specific volume of ice and ΔH_{F} is latent heat of fusion of water. We write the radius of curvature of the ice particle as:

$$r = \frac{r_0}{\ln\left(\frac{T_0}{T}\right)} \tag{2}$$

where $r_0 = \dfrac{2\sigma V}{\Delta H_{\mathrm{F}}}$.

Thus, Eq. (2) represents the ice formation in the presence of water. We consider that r_0 is a function of the interfacial free energy between the ice and the surrounding liquid, the molar latent heat of fusion and the specific molar volume of ice. But here we used it as a free parameter, to take into account that ice forms gradually as the temperature decreases below 0 °C. T_0 is equal to 273 K for pure water, but due to the presence of soluble solids in the juice, its value for juice is lower and close to the eutectic temperature. The ice/water interface has a curvature given by the radius r. Thus, the functional form given by Eq. (2) is used to obtain the radius of the capillary pore using r_0 and T_0 as free parameters to fit the experimental data. We obtain the proportion of unfrozen water, ϕ_{w}, versus temperature by using a Gaussian distribution for the size of the ice particles. That is, using Eq. (2), we obtain:

$$\phi_{\mathrm{w}} = \frac{A}{\Delta r\sqrt{2\pi}}\int_0^{r_0/\ln(T_0/T)} \mathrm{e}^{\frac{-(r-r_{\mathrm{av}})^2}{2\Delta r^2}}\,\mathrm{d}r \tag{3}$$

where r_{av} is the average radius, Δr is the standard deviation, and the temperature T is given in Kelvin. The quantity $r_0 = 0.228$ nm for the ideal case (Leclaire et al., 1994). The constant A is obtained after normalization of the Gaussian function from $r = 0$ to $r = \infty$. Thus, the amount of unfrozen water as function of the temperature can be calculated as:

$$\phi_{\mathrm{w}}(T) = \frac{\mathrm{erf}(\zeta) + \mathrm{erf}(\gamma)}{1 + \mathrm{erf}(\gamma)}; \quad \zeta = \frac{\frac{r_0}{\ln\frac{T_0}{T}}}{\sqrt{2}\Delta r}; \quad \gamma = \frac{r_{\mathrm{av}}}{\sqrt{2}\Delta r} \tag{4}$$

2.2. Wave-velocity model

First, we obtain the shear and bulk moduli of the matrix formed by the ice phase as:

$$\mu_{\mathrm{m}} = \mu_{\mathrm{i}}(1-\phi_{\mathrm{w}})^{3.8} \tag{5}$$

$$K_{\mathrm{m}} = K_{\mathrm{i}}(1-\phi_{\mathrm{w}})^{3.8} \tag{6}$$

where μ_{i} and K_{i} are the shear and bulk moduli of ice, respectively. Eq. (5) is a percolation model of ice formation (Leclaire et al., 1994). Arbabi and Sahimi (1988) performed numerical simulations of elastic properties of three-dimensional percolation networks and using Monte Carlo simulations and finite-size scaling analysis, they found that the exponent of Eqs. (5) and (6) should be 3.78 with an error of about 3%. This exponent is a critical value that characterizes the power-law behavior of the elastic moduli near the percolation threshold.

The density of the frozen porous medium is:

$$\rho = (1-\phi_{\mathrm{w}})\rho_{\mathrm{i}} + \phi_{\mathrm{w}}\rho_{\mathrm{w}} \tag{7}$$

where ρ_{i} and ρ_{w} are the ice and water densities, respectively. Hence, according to Biot's theory, the low-frequency shear-wave velocity is:

$$v_{\mathrm{S}} = \sqrt{\frac{\mu_{\mathrm{m}}}{\rho}} \tag{8}$$

The low-frequency bulk modulus of the partially frozen medium is given by the Gassmann's modulus as:

$$K_{\mathrm{G}} = \frac{K_{\mathrm{i}} - K_{\mathrm{m}} + \phi_{\mathrm{w}}K_{\mathrm{m}}(K_{\mathrm{i}}/K_{\mathrm{w}} - 1)}{1 - \phi_{\mathrm{w}} - K_{\mathrm{m}}/K_{\mathrm{i}} + \phi_{\mathrm{w}}K_{\mathrm{i}}/K_{\mathrm{w}}} \tag{9}$$

where K_{w} is the bulk modulus of water.

The low-frequency P-wave velocity is

$$v_{\mathrm{P}} = \sqrt{\frac{K_{\mathrm{G}} + 4/3\mu_{\mathrm{m}}}{\rho}} \tag{10}$$

A more convenient model is given by using the high-frequency Biot's theory because the experimental data from Lee et al. (2004) was obtained at a frequency of 5 MHz. This theory provides complex velocities, from which the phase velocities and attenuation factors can be obtained (Biot, 1962; Carcione, 2001). Johnson et al. (1987) obtained an expression for the correction term to be applied at high frequencies due to deviations of the fluid flow from the Poiseuille (laminar) flow. They obtained an expression for the dynamic tortuosity, which provides a good description of both the magnitude and phase of the exact dynamic tortuosity of large networks formed from a distribution of random radii. For shear waves, the phase velocity and attenuation factor are:

$$v_{\mathrm{s}} = \frac{1}{\mathrm{Re}\left(\frac{1}{v_{\mathrm{c}}^{\mathrm{s}}}\right)} \tag{11}$$

and

$$\alpha_{\mathrm{s}} = \omega\,\mathrm{Im}\left(\frac{1}{v_{\mathrm{c}}^{\mathrm{s}}}\right) \tag{12}$$

where the complex velocity $v_{\mathrm{c}}^{\mathrm{s}}$ can be calculated as:

$$v_{\mathrm{c}}^{\mathrm{s}} = \sqrt{\frac{\mu_{\mathrm{m}}}{\rho - \frac{\mathrm{i}\omega\rho_{\mathrm{w}}^2}{Y(\omega)}}} \tag{13}$$

ω is the angular frequency ($\omega = 2\pi f$) and Re and Im are the real and complex parts of a complex number. The quantity

$Y(\omega)$ in Eq. (13) is a viscodynamic term, which is important at high frequencies. It is given by:

$$Y(\omega) = \mathrm{i}\omega\left(\frac{\rho_{\mathrm{w}}\tau}{\phi_{\mathrm{w}}}\right) + \frac{\eta F(\omega)}{\kappa} \tag{14}$$

where η is the water viscosity, τ is the tortuosity of the pore space, given by:

$$\tau = 1 + \beta\left(\frac{1}{\phi_{\mathrm{w}}} - 1\right) \tag{15}$$

with $\beta = 1/2$ for spherical grains, and κ is the permeability, given by the Kozeny–Carman relation (Mavko, Mukerji, & Dvorkin, 1998):

$$\kappa = \frac{2\kappa_0\phi_{\mathrm{w}}^3}{(1-\phi_{\mathrm{w}})^2} \tag{16}$$

where κ_0 is a reference value at 50% water proportion; in this work we used the value of 2.5 Darcy which is a value commonly used for materials with relatively high porosity like frozen foods. The viscosity correction term $F(\omega)$ is given by:

$$F(\omega) = \sqrt{1 - \frac{4\mathrm{i}\tau^2\kappa}{x\Lambda^2\phi_{\mathrm{w}}}}, \quad x = \frac{\eta\phi_{\mathrm{w}}}{\omega\kappa\rho_{\mathrm{w}}} \tag{17}$$

where Λ is a geometrical parameter, with $2/\Lambda$ being the surface-to-pore volume ratio of the pore-solid interface. The following relation between τ, κ, and Λ can be used:

$$\frac{\xi\tau\kappa}{\phi_{\mathrm{w}}\Lambda^2} = 1 \tag{18}$$

where $\xi = 12$ for a set of canted slabs of fluid, and $\xi = 8$ for a set of non-intersecting canted tubes.

The complex velocity of the P-waves can be obtained from the following fourth-order equation:

$$av_{\mathrm{c}}^{\mathrm{p}4} + bv_{\mathrm{c}}^{\mathrm{p}2} + c = 0 \tag{19}$$

where

$$a = -\left(\rho_{\mathrm{w}}^2 + \frac{\mathrm{i}}{\omega}Y(\omega)\rho\right) \tag{20}$$

$$b = \frac{\mathrm{i}}{\omega}Y(\omega)E_{\mathrm{G}} + M(2\alpha\rho_{\mathrm{w}} - \rho) \tag{21}$$

and

$$c = ME_{\mathrm{m}} \tag{22}$$

The parameters E_{m}, E_{G} and α are the P-wave modulus of the ice frame, the Gasmann P-wave modulus and the Biot effective stress coefficient respectively, which can be calculated as:

$$E_{\mathrm{m}} = K_{\mathrm{m}} + \frac{4}{3}\mu_{\mathrm{m}} \tag{23}$$

$$E_{\mathrm{G}} = K_{\mathrm{G}} + \frac{4}{3}\mu_{\mathrm{m}} \tag{24}$$

$$\alpha = 1 - \frac{K_{\mathrm{m}}}{K_{\mathrm{i}}} \tag{25}$$

whereas the parameter M can be calculated as:

$$M = \frac{K_{\mathrm{i}}}{1 - \phi_{\mathrm{w}} - K_{\mathrm{m}}/K_{\mathrm{i}} + \phi_{\mathrm{w}}K_{\mathrm{i}}/K_{\mathrm{w}}} \tag{26}$$

The solution of Eq. (19) has two roots, corresponding to the fast and slow P-waves. Let us denote the respective complex velocities by $v_{\mathrm{c}}^{\mathrm{p}\pm}$, where the signs correspond to the signs of the square root resulting from the solution of Eq. (19). The phase velocities are then:

$$v_{\mathrm{P}\pm} = \frac{1}{\mathrm{Re}\left(\frac{1}{v_{\mathrm{c}}^{\mathrm{p}\pm}}\right)} \tag{27}$$

and the attenuation factors are:

$$\alpha_{\mathrm{P}\pm} = -\omega\,\mathrm{Im}\left(\frac{1}{v_{\mathrm{c}}^{\mathrm{p}\pm}}\right) \tag{28}$$

3. Results

The properties used in the calculations are given in Table 1. The high viscosity value used (100 times the viscosity of liquid water) is due to the presence of sugars in the liquid and the low temperature. Fig. 1 shows the proportion of water versus temperature, where the symbols correspond to the experimental data, obtained by using a NMR-based technique (Lee et al., 2004), and the trace of the solid line are the results obtained from Eq. (4). At −10 °C orange juice still contains a significant portion of the juice (unfrozen water) in a liquid state; below this temperature, more ice crystals will form. NMR data shows that unfrozen water ϕ_{w} is approximately 15% at $T = -20$ °C and $\phi_{\mathrm{w}} = 5\%$ at $T = -50$ °C. The calculated P-wave and S-wave velocities at 5 MHz are compared to the experimental data in Fig. 2. In order to obtain a good fit of the velocities, the moduli of the fully frozen orange juice slightly differ from that of pure ice ($K_{\mathrm{i}} = 8.5$ GPa and $\mu_{\mathrm{i}} = 3.7$ GPa) as those indicated in Table 1. This can be justified on the basis that the presence of pulp particles modifies the frozen juice or ice true moduli.

Fig. 3 shows the calculated P-wave attenuation factor at 5 MHz, compared to the experimental data. There is a

Table 1
Material properties

Ice bulk modulus, K_{i}	10.3 GPa
Ice shear modulus, μ_{i}	4 GPa
Ice density, ρ_{i}	920 kg/m^3
Water bulk modulus, K_{w}	2.25 GPa
Water density, ρ_{w}	1030 kg/m^3
Water viscosity, η	0.1 Pa s
Matrix permeability, κ_0	2.5 Darcy
Juice eutectic temperature, T_{e}	−10 °C
Average radius, r_{av}	10 μm
Standard deviation, Δr	10 μm
r_0	0.228 μm
β	0.02
ξ	8

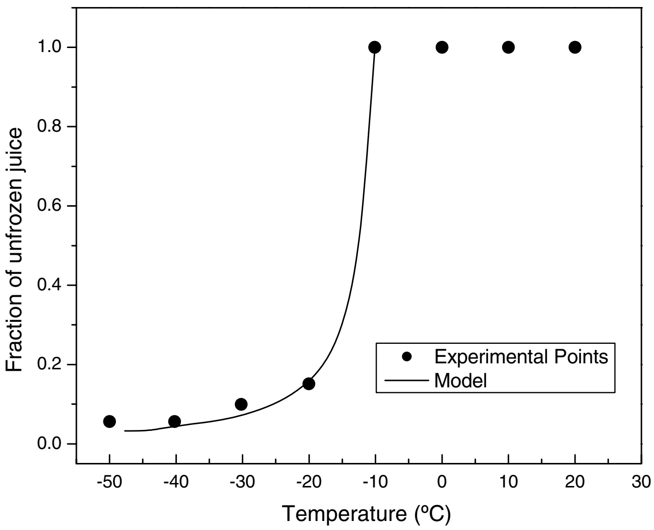

Fig. 1. Proportion of unfrozen juice as a function of temperature. The symbols correspond to the experimental data (Lee et al., 2004).

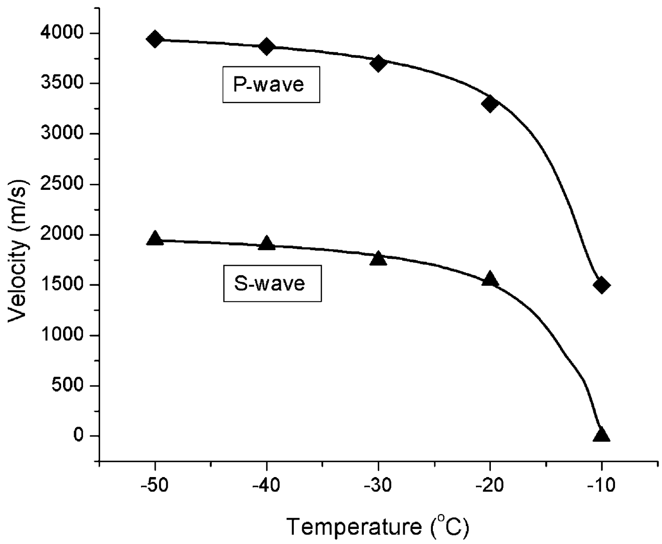

Fig. 2. P-wave and S-wave velocities as a function of temperature. The symbols correspond to the experimental data (Lee et al., 2004).

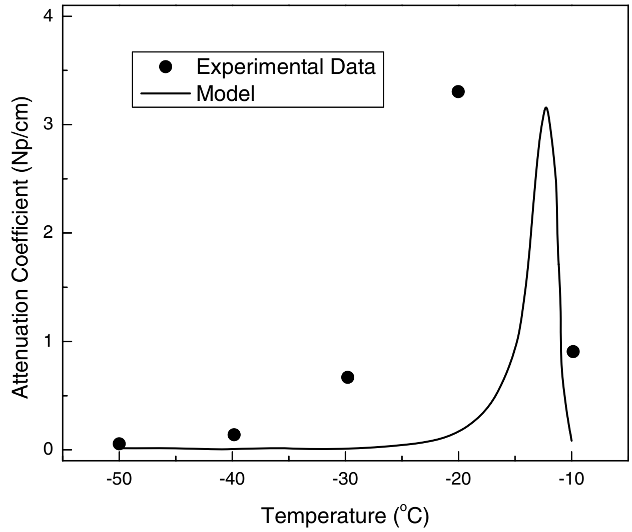

Fig. 3. P-wave attenuation coefficient as a function of temperature. The symbols correspond to the experimental data (Lee et al., 2004).

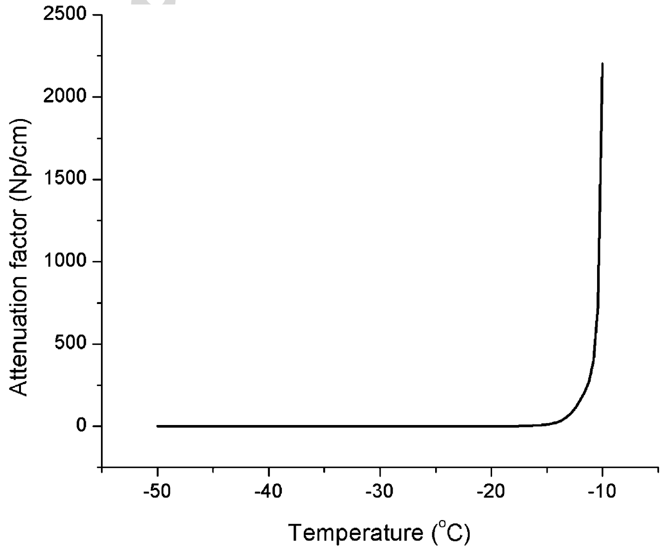

Fig. 4. S-wave attenuation coefficient as a function of temperature.

qualitative similarity between the curves, although the peak temperatures do not coincide. The theoretical peak temperature corresponds to 50% water saturation (50% ice content). In order to fit the experimental data, the reference permeability κ_0, ξ and β have been chosen as shown in the table. These values imply relatively low values of the permeability and tortuosity of the matrix. It is highly probably that patchy inhomogeneities and scattering effects play an important role, and that the attenuation due to the Biot mechanism partially describes the observed dissipation. The inhomogeneities not only cause scattering of the P-waves but also are responsible of the mesoscopic mechanism by which fast P-wave energy is converted to slow P-wave energy (fluid-pressure energy diffusion) (White, 1975; Carcione, Helle, & Pham, 2003a; Pride, Berryman, & Harris, 2004). Moreover, a refinement of the model requires a better description of the effect of temperature on viscosity using the Arrhenius equation (Fergurson & Kemblowski, 1991), and the fact the decreasing temperatures implies increasing viscosity due to increasing sugar concentrations in the unfrozen juice solution.

Fig. 4 shows the calculated attenuation factor of the shear wave, which is quite significant at the eutectic temperature. For completeness, in Fig. 5, we show the calculated phase velocity (a) and the attenuation factor of the slow P-wave. The velocity has a maximum and the attenuation a minimum at nearly −12 °C and 50% saturation, which seems to be a critical saturation of the partially saturated medium. Despite the wave-like features of the slow P-wave, its attenuation is very high, indicating a strong diffusive character of the system. These characteristics indicate why the slow P-wave cannot be observed in the experiments.

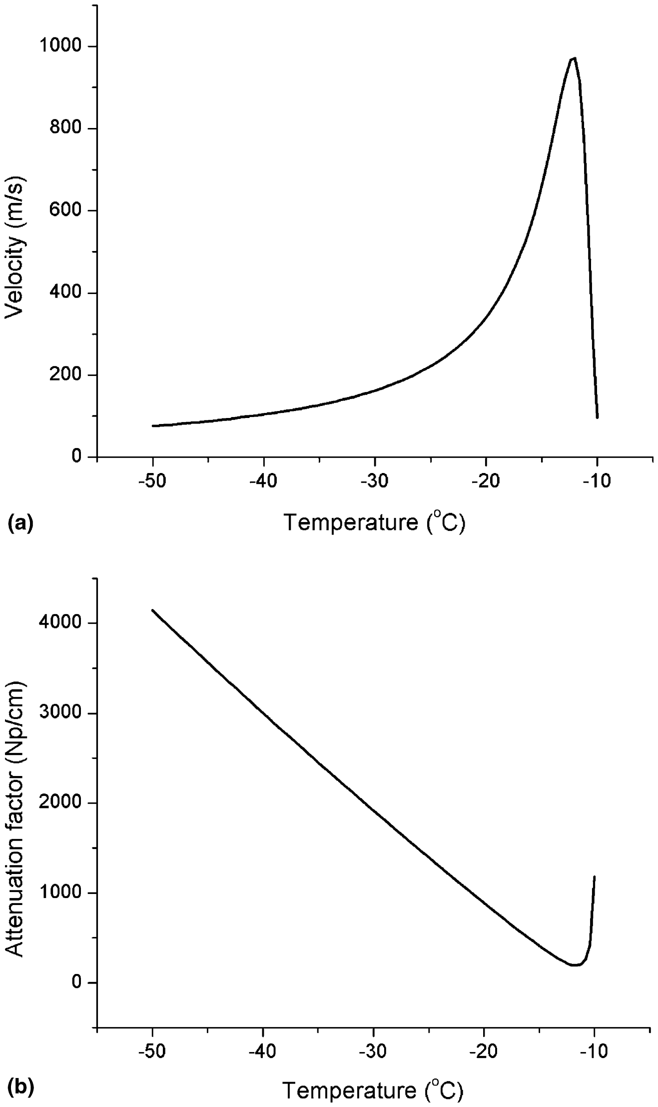

Fig. 5. Velocity (a) and attenuation coefficient (b) of the slow P-wave.

4. Conclusions

We have developed a poroelastic model to predict the degree of freezing of orange juice by means of the wave velocity and attenuation factor. The adjustable parameters of the model are the average radius and standard deviation of the pores (i.e. the porous structure of the material) that are used to obtain the liquid saturation. In addition the stiffness moduli of the frozen juice to obtain the wave velocities (although as expected these moduli did not significantly differ from those of pure ice) and the viscosity of the juice and permeability of the ice frame are used to obtain the maximum P-wave attenuation. The model shows an excellent agreement with the experimental data, particularly, the ultrasonic velocities. The attenuation curve of the compressional wave shows a qualitative agreement with the experimental curve, predicting a critical temperature at 50% saturation, for which the dissipation is maximum. In addition, the model provides the properties of the slow compressional wave, which shows a diffusive character at ultrasonic frequencies.

Further research to improve the description of the attenuation mechanisms involves a better characterization of the liquid viscosity as a function of temperature and the modeling of the mesoscopic-loss mechanism. The viscosity-temperature relationship of the fluid (juice) can be expressed in the form of an Arrhenius equation. Moreover, since the solids concentration in the juice increases with decreases in temperature, viscosity should also increase. Regarding the mesoscopic-loss mechanism, Biot's theory for homogeneous media is often reported to underestimate velocity dispersion and attenuation. As shown by White (1975), these quantities are substantially affected by the presence of partial (patchy) saturation. In our case, heterogeneities (patches) in the different properties of the medium may cause the mesoscopic loss (fluid-pressure energy diffusion by slow-wave conversion to fast P-wave), and scattering attenuation, which is not described by Biot's theory, but can be modeled by means of numerical simulations (Carcione, Santos, Ravazzoli, & Helle, 2003b).

References

Arbabi, S., & Sahimi, M. (1988). Elastic properties of three-dimensional percolation networks with stretching and bond-bending forces. *Physical Review B, 38*, 7173–7176.

Biot, M. A. (1956). Theory of propagation of elastic waves in a fluid-saturated porous solid. I. Low-frequency range. *Journal of the Acoustical Society of America, 28*, 168–178.

Biot, M. A. (1962). Mechanics of deformation and acoustic propagation in porous media. *Journal of Applied Physics, 33*, 1482–1498.

Carcione, J. M. (2001). *Wave fields in real media: wave propagation in anisotropic, anelastic and porous media. Handbook of geophysical exploration* (Vol. 31). Pergamon Press Inc.

Carcione, J. M., Helle, H. B., & Pham, N. H. (2003a). White's model for wave propagation in partially saturated rocks: comparison with poroelastic numerical experiments. *Geophysics, 68*, 1389–1398.

Carcione, J. M., Santos, J. E., Ravazzoli, C. L., & Helle, H. B. (2003b). Wave simulation in partially frozen porous media with fractal freezing conditions. *Journal of Applied Physics, 94*, 7839–7847.

Fergurson, J., & Kemblowski, Z. (1991). *Applied fluid rheology*. London: Elsevier Applied Science.

Hartel, R. (1998). Mechanisms and kinetics of recrystallization in ice cream. In D. Reid (Ed.), *The properties of water in foods*. Blackie Academic and Professional.

Hudson, J. (1992). *Surface science, an introduction*. Boston: Butterworth-Heinemann.

Johnson, D. L., Koplik, J., & Dashen, R. (1987). Theory of dynamic permeability and tortuosity in fluid-saturated porous media. *Journal of Fluid Mechanics, 176*, 379–402.

Karel, M., & Lund, D. B. (2003). Freezing. In *Physical principles of food presevartions*. New York: Marcel Dekker.

Leclaire, Ph., Cohen-Ténoudji, F., & Aguirre-Puente, J. (1994). Extension of Biot's theory of wave propagation to frozen porous media. *Journal of Acoustical Society of America, 96*, 3753–3768.

Lee, S., Pyrak-Nolte, L. J., Cornillon, P., & Campanella, O. H. (2004). Characterization of frozen orange juice by ultrasound and wavelet analysis. *Journal of the Science of Food and Agriculture, 84*, 405–410.

Mavko, G., Mukerji, T., & Dvorkin, J. (1998). *The rock physics handbook: tools for seismic analysis in porous media*. Cambridge University Press.

McClements, D. J., & Povey, M. J. W. (1987). Solid fat content determination using ultrasonic velocity measurements. *International Journal of Food Science and Technology, 22*, 419–428.

Miles, C. A., & Cutting, C. L. (1974). Changes in the velocity of ultrasound in meat during freezing. *Journal of Food Technology, 9*, 119–122.

Povey, M. (1997). *Ultrasonic techniques for fluids characterization*. Academic Press.

Povey, M., & Mason, T. (1995). *Ultrasound in food processing*. Kluwer Academic.

Pride, S. R., Berryman, J. G., & Harris, J. M. (2004). Seismic attenuation due to wave- induced flow. *Journal of Geophysical Research, 109*, B01201. doi:10.1029/2003JB002639.

Sigfusson, H., Ziegler, G. R., & Coupland, J. N. (2004). Ultrasonic monitoring of food freezing. *Journal of Food Engineering, 62*, 269–363.

Singh, P. R. (1995). Thermal properties of frozen foods. In M. A. Rao & S. S. H. Rizvi (Eds.), *Engineering properties of foods* (2nd ed.). New York: Marcel Dekker.

White, J. E. (1975). Computed seismic speeds and attenuation in rocks with partial gas saturation. *Geophysics, 40*, 224–232.